



The intrinsically disordered RNR inhibitor Sml1 is a dynamic dimer

Danielsson, Jens; Liljedahl, Leena; Bárány-Wallje, Elsa; Sønderby, Pernille; Kristensen, Line Hyltoft; Martinez-Yamout, Maria; Dyson, H. Jane; Wright, Peter E.; Poulsen, Flemming M.; Måler, Lena

Total number of authors:
12

Published in:
Biochemistry

Link to article, DOI:
[10.1021/bi801040b](https://doi.org/10.1021/bi801040b)

Publication date:
2008

Document Version
Peer reviewed version

[Link back to DTU Orbit](#)

Citation (APA):

Danielsson, J., Liljedahl, L., Bárány-Wallje, E., Sønderby, P., Kristensen, L. H., Martinez-Yamout, M., Dyson, H. J., Wright, P. E., Poulsen, F. M., Måler, L., Gråslund, A., & Kragelund, B. B. (2008). The intrinsically disordered RNR inhibitor Sml1 is a dynamic dimer. *Biochemistry*, 47(50), 13428-13437. <https://doi.org/10.1021/bi801040b>

General rights

Copyright and moral rights for the publications made accessible in the public portal are retained by the authors and/or other copyright owners and it is a condition of accessing publications that users recognise and abide by the legal requirements associated with these rights.

- Users may download and print one copy of any publication from the public portal for the purpose of private study or research.
- You may not further distribute the material or use it for any profit-making activity or commercial gain
- You may freely distribute the URL identifying the publication in the public portal

If you believe that this document breaches copyright please contact us providing details, and we will remove access to the work immediately and investigate your claim.



Published in final edited form as:

Biochemistry. 2008 December 16; 47(50): 13428–13437.

The intrinsically disordered RNR inhibitor Sml1 is a dynamic dimer

Jens Danielsson^{1,2}, Leena Liljedahl², Elsa Bárány-Wallje¹, Pernille Sønderby², Line Hyltoft Kristensen², Maria Martinez-Yamout³, H. Jane Dyson³, Peter E. Wright³, Flemming M. Poulsen², Lena Måler¹, Astrid Gråslund¹, and Birthe B. Kragelund²,

¹Department of Biochemistry and Biophysics, Stockholm University, S-106 91 Stockholm Sweden;

²Structural Biology and NMR Laboratory, Department of Biology, University of Copenhagen, Ole Maaloes Vej 5, DK-2200 Copenhagen N, Denmark;

³Department of Molecular Biology and Skaggs Institute for Chemical Biology, The Scripps Research Institute, 10550 North Torrey Pines Rd, La Jolla, CA 92037, USA

Abstract

Sml1 is a small ribonucleotide reductase (RNR) regulatory protein in *Saccharomyces cerevisiae* that binds to and inhibits RNR activation. NMR studies of ¹⁵N-labeled Sml1 (104 residues), as well as of a truncated variant (residues 50-104), have allowed characterization of their molecular properties. Sml1 belongs to the class of intrinsically disordered proteins with high degree of dynamics and very little stable structures. Earlier suggestions for a dimeric structure of Sml1 were confirmed and from translation diffusion NMR measurements a dimerization dissociation constant of 0.1 mM at 4 °C could be determined. The hydrodynamic radius for the monomeric form of Sml1 was determined to be 23.4 Å corresponding to a protein size in between a globular protein and a coil. The dimer formation results in a hydrodynamic radius of 34.4 Å. The observed chemical shifts showed in agreement with previous studies two segments with transient helical structure, residues 4-20 and 60-86, and relaxation studies clearly showed restricted motion in these segments. A spin label attached to C14 showed long range interactions with residues 60-70 and 85-95, suggesting that the N-terminal domain folds onto the C-terminal domain. Importantly, protease degradation studies combined with mass-spectrometry indicated that the N-terminal domain is degraded before the C-terminal region and thus may serve as a protection against proteolysis of the functionally important C-terminal region. The dimer formation was not associated with significant induction of structure, but was found to provide further protection against proteolysis. We propose that this molecular shielding and protection of vital functional structures from degradation by functionally unimportant sites may be a general attribute of other natively disordered proteins.

Keywords

IDP; NMR; protein folding; relaxation; diffusion

The suppressor of Mec1 lethality (Sml1) is a small ribonucleotide reductase (RNR) regulatory protein in *Saccharomyces cerevisiae* that binds to and inhibits RNR activation. The highly conserved RNR reduces the ribonucleotides to deoxyribonucleotides necessary for DNA synthesis and in yeast it is a heterotetramer of one homodimer, the R1 and the heterodimer R2-R4 proteins (1,2). Sml1 binds specifically to the R1 component of RNR in a one-to-one

*Corresponding author. Email address: bbk@bio.ku.dk, Phone: +45 35 32 20 81; Fax: +45 35 32 21 28.

SUPPORTING INFORMATION: Normalized peak height of ¹H, ¹⁵N-HSQC of the Sml1 sample versus 10X/1RED ratios of the ¹⁵N-Sml1-MTSL sample with peak heights measured from a ¹H, ¹⁵N-HSQC spectra (Figure S1). Size exclusion chromatography profiles of Sml1 (Figure S2). This material is available free of charge at the internet at <http://pubs.acs.org>

stoichiometry with a dissociation constant in the low micromolar regime (3,4) and at an RNR R1:Sml1 ratio of 1:1 50% inhibition is achieved (3). RNR is particularly active during the S-phase of the cell cycle. Its activity is regulated on different levels. In *S. cerevisiae* one of the regulatory mechanisms is via Sml1. First, the expression level of Sml1 is decreased during the S-phase of the cell cycle (5,6). Second, a posttranslational modification of Sml1, i.e. by phosphorylation of one or more of the serines S56, S58 and S60, leads to degradation of Sml1, and this constitutes a second level of regulation (5,7). S60 seems to be the most potent regulation site, since it is phosphorylated to the greatest extent of the three. Sml1 regulation of RNR activity is not only seen during normal DNA synthesis but also as a response to DNA damage (5,8,9).

Sml1 is a small protein of 104 residues, and its sequence (shown in Figure 1A) suggests that it is mostly unstructured and belongs to the group of intrinsically disordered proteins (IDP) (10,11). Sml1 has however been suggested to adopt transient structures in three regions along the chain, two in the N-terminal part of the protein, involving residues 4-14 and 20-35, and one in the C-terminal part involving residues 61-80. Between these more structured regions the polypeptide chain is essentially random in structure (12). The regions 4-14 and 61-80 have high propensities to adopt transient α -helical conformation, although no well defined helical structures have been determined. Mutation/deletion-studies of Sml1 suggest that the C-terminal helical region is important for Sml1 inhibition of RNR (12). Helix breaking mutations inside this region, such as S75P, reduce the inhibitory effect of Sml1 significantly. However, mutations outside the helical region, but still in the C-terminal region also decrease Sml1 inhibitory efficiency significantly. Together with the observation that replacement of the C-terminal F104 for a Leu leads to a considerable reduction in inhibition, this suggests that a large part of the C-terminus of Sml1 is important for its inhibitory function. Even a short peptide with the same sequence as the nine C-terminal residues of Sml1 inhibits RNR activity to some extent. In contrast, deletion of several N-terminal parts of Sml1 had no effect on RNR R1 inhibition (12), indicating that the N-terminal region is probably not important for Sml1 function.

Sml1 has been suggested to form a stable dimer and initially a disulphide bridge was assumed to form between C14 of the monomers (7). However, mutation studies showed that a dimer was formed even in the absence of the cysteine, suggesting the presence of important intermolecular non-covalent interactions. Since truncation of the outermost 20 N-terminal residues reduced and even eliminated the presence of dimers (13), the N-terminal part of Sml1 may control this process.

IDPs are an important group of proteins, typically involved in regulation of transcription, translation and cell signaling (10). Upon interaction with functional partners, which themselves may be folded or unfolded, IDP domains frequently undergo binding-coupled folding (10). The induced structure is often directly related to structural propensities already present in the unbound disordered state. Nuclear magnetic resonance spectroscopy (NMR) is the method of choice for structural and dynamical characterization of such disordered peptide chains (14-17), and the results can mostly be substantiated by information obtained by other biophysical methods such as circular dichroism, fluorescence and mass spectrometry (18-19).

Previous NMR studies have shown that the peptide backbone of Sml1 has two regions (4-14) and (61-80) with high α -helix propensities, and relaxation studies have shown that the backbone structure is highly flexible at pH 7.0 with S^2 order parameters all below 0.6 (12). The two helices were suggested to interact with each other and to run anti-parallel. By mapping solvent protected side chains of Sml1, it was also suggested to adopt a solvent-excluding three-dimensional structure (20). However, no detailed analysis was reported of the structural and dynamical characteristics of Sml1 in solution and no information regarding details of the

dimerization of Sml1 has been reported. In this work, we have characterized in detail the structure and dynamics of Sml1 using a variety of biophysical methods. We have also specifically studied and characterized the dimerization in terms of the dissociation constant and have identified residues important for dimerization. Furthermore we have resolved a likely biological role of the N-terminal region.

It is a challenge to couple the structural susceptibilities and the dynamic properties of a protein to its functional state, particularly when the functional bound state is not yet known, as for Sml1. Here we have used truncation as a strategy to correlate the structural and dynamical properties of Sml1 to its function. This is important in the ongoing work to understand Sml1 binding and inhibition of RNR, and to the understanding and subsequently the manipulation of the potential regulation of eukaryotic RNR.

EXPERIMENTAL PROCEDURES

Protein expression and purification

The *S.cerevisiae* WT *SML1* gene was cloned into the pET-3a vector between the restrictions sites BamH1 and Nde1. In order to control the cloning was correct, the plasmid was cut by the restriction enzymes BamH1 and Nde1 and PCR amplification of the insert was performed. BL21(DE3) and BL21(DE3) pLysS competent *E.coli* cells were used for the IPTG induced expression of Sml1 from vector pET-3a. Recombinant wild type Sml1 and the studied variants of Sml1 were expressed as described by Chabes et al (3). Cells were harvested after 4 hours by centrifugation, resuspended in 50 mM Tris-HCl, pH 7.4, 1 mM EDTA, and lysed by sonication 3 × 30 sec on ice. The cells were centrifuged at 20.000 × g for 25 min at 4°C. Proteins in the supernatant were precipitated by adding solid ammonium sulphate to 25% saturation at 0°C (136 g/l) and centrifuged at 12.000 × g for 15 min at 4°C. The supernatant was carefully removed, and the pellet dissolved in 10 mM Tris-HCl, pH 8.0 (RPC-buffer A). Further purification was done using reverse phase HPLC with application of a SOURCE 15 RPC ST 4.6/100 column. Aliquots of protein were injected onto the column, and Sml1 eluted in a linear gradient in RPC-buffer B (10 mM Tris-HCl pH 8.0, 60% MeCN), increasing from 25-60 %B (v/v) over 10 column volumes, flow rate 1 ml/min.

Spectroscopic methods

All experiments were performed at 4°C and pH 7 (6.9-7.4) in 10 mM phosphate buffer. C α , CO, N and HN chemical shifts of ¹³C and ¹⁵N labeled Sml1 were recorded at pH 7, 4 °C and 0.6 mM concentration using standard ¹⁵N-HSQC, HNCA, HN(CO)CA, HNCACB, CBCACONH, HN(CA)CO and HNCO experiments on a Varian Inova 800 MHz spectrometer equipped with a cryogenically cooled triple resonance probe. Spectra were processed using nmrPipe and analyzed using the programs Sparky (T. D. Goddard and D. G. Kneller, SPARKY 3, UCSF) and Pronto (21).

Diffusion experiments were performed using a PFG-LED sequence with a gradient pre pulse (22-23) on a Varian Inova 750 MHz spectrometer. The ¹H signal intensity was determined at 24 linearly spaced gradient strengths and the attenuating intensity was fitted to a modified Stejskal-Tanner equation where nonlinearities in the gradient field profile are accounted for (24-25). The signal intensity was measured on methyl groups and aromatics separately. The diffusion delay was 150 ms and the gradient pulses was 5 ms. The hydrodynamic radius was calculated using Stokes-Einstein's expression, and was determined three times at each concentration. The dilution series was performed using a high concentration sample that was diluted in several steps, and the diffusion coefficient was determined after a 1-2 h delay, necessary to achieve an equilibrium state. The fitting routine was performed using MATLAB (Mathworks, Natick, MA, USA). The gradient was calibrated using the HDO and α cyclodextrin

diffusion at 4°C ($10.5 \cdot 10^{-10}$ and $1.46 \cdot 10^{-10}$ m²/s respectively). The concentration dependence of the hydrodynamic radii were fitted to a model with an equilibrium between monomer, M, and dimer, D, assuming that the exchange between these states is fast on the diffusion timescale,



The dissociation constant, K_D , is the ratio of the equilibrium concentrations of monomers and dimers.

$$K_D = [M]^2 / [D] = (C_0 p_{\text{monomer}})^2 / \frac{1}{2} C_0 (1 - p_{\text{monomer}}) \quad (2)$$

Here C_0 is the total protein concentration and p_{monomer} is the monomer population. At each concentration the population of monomer can be determined as the weighted mean of the observed diffusion coefficient.

$$D_{\text{obs}} = p_{\text{monomer}} D_{\text{monomer}} + (1 - p_{\text{monomer}}) D_{\text{dimer}} \quad (3)$$

By combining equations 1-3 and determining D_{obs} at several concentrations C_0 , K_D , D_{monomer} and D_{dimer} may be obtained from a nonlinear fit. This was performed using MATLAB.

The relaxation experiments were performed using standard HSQC sequences and at three different fields 500 MHz (Bruker Avance, Karlsruhe, Germany), 600 and 800 MHz (Varian Inova, Palo Alto, CA, USA) proton frequency field. The signal attenuation, from 10 different relaxation delays, was fitted to a single exponential decay and the relaxation rates were determined. The relaxation rates were determined at high protein concentration, 0.7 mM.

Paramagnetic relaxation enhancement experiments were performed as described earlier and Sml1 was spin labeled with MTSL as described (26). The labeled and the unlabeled fractions were separated using reverse phase high pressure liquid chromatography. The MTSL spin label was reduced using four times molar excess of ascorbic acid and readjusting pH.

Determination of hydrodynamic radius by gel filtration

Samples of WT-SM11 were analyzed at different concentrations (9.8 mM and 0.8 mM) using an ÄKTA HPLC purifier on a pre-packed Superdex G75 10/300 Tricorn High performance column with a V_t of 24 mL with a 20 mM Tris-HCl, pH 7.5, 150 mM NaCl, flow rate 0.5 ml/min. The column was calibrated using ovalbumin (43 kDa, 30Å), myoglobin (17 kDa, 17Å), BSA (66 kDa, 35.5 Å) α -chymotrypsinogen A (25 kDa, 20.9Å) and ribonuclease A (13.7 kDa, 16.4Å), as well as blue dextran (V_0) and acetone (V_t). K_{AV} was calculated from $K_{AV} = (V_e - V_0) / (V_t - V_0)$, where V_e is the elution volume of each protein.

Protease resistance

Protease K and trypsin proteomics grade was purchased from Sigma Aldrich (St Louis, MO, USA) and used without further purification. The protease K assays were carried out in 50 mM Tris-HCl pH 8, 5 mM CaCl₂ at room temperature. Protease K was added to protein samples in a molar ratio 1:10000. Aliquots of the protein-protease K mixture were withdrawn after varying delays, and the reaction stopped by adding PMSF to a final concentration of 5 mM. Aliquots were analyzed using SDS-PAGE. Limited trypsin digestion was carried out in 100 mM NH₄HCO₃, pH 7.4 at room temperature. Trypsin was added to the protein samples in a molar ratio of 1:2000. Aliquots of protein-trypsin mixture were withdrawn after 0, 5, 10, 20 or

40 min, and the reactions stopped by adding TFA to a final concentration of 1 % (v/v). Samples were analysed with SDS-PAGE or MALDI-TOF MS.

MALDI-TOF MS

1 μ l of 20 μ M digest was mixed with 1 μ l HCCA (10 mg/ml in 50% (v/v) MeCN, 0.1% (v/v) TFA) and spotted on a MTP 384 ground steel TF target plate by the dried droplet method. Spectra were recorded on a Bruker Daltonics Autoflex II TOF mass spectrometer in linear positive mode. An average of 100 shots was recorded. Calibration was performed with quadric calibration of either protein calibration standard 1 or peptide calibration standard (both purchased from Bruker Daltonics). Spectra were analysed with MoverZ (Proteometrics, Inc). Primary sites were identified from two corresponding fragments giving the full sequence.

RESULTS

Structural characterization

A number of NMR spectroscopy experiments were performed in order to elucidate the residual secondary structure of Sml1 and the oligomeric state of the protein. The ^1H , ^{15}N -heteronuclear single quantum correlation (HSQC) spectra of Sml1 at a wide range of concentrations were well resolved; cross-peaks corresponding to 96 of 99 non-proline residues have been assigned. The assignment is in general agreement with earlier findings (12) with a few exceptions. The small spectral width of the amide signals of Sml1 clearly indicates that the protein is mainly unfolded as was predicted also from the sequence properties.

Hydrodynamic dimensions of Sml1

From the hydrodynamic radius it is possible to distinguish between the presence of folded and unfolded protein in a sample (16,27-28) and between monomeric and dimeric protein. It has been suggested that Sml1 exists as a dimer (13). Assuming that the protein is in equilibrium between monomeric and dimeric states and that the exchange between these states are fast at the diffusion time scale, NMR pulsed field gradient (PFG) diffusion experiments in a dilution series should give direct evidence on such an equilibrium (24,27-28). Figure 1B shows the attenuation curves from Sml1 at 4 °C in D_2O at two different concentrations, 550 μM and 25 μM . It is immediately clear that Sml1 diffuses significantly faster at low concentration. We performed a dilution series, and determined the hydrodynamic radius at several concentrations. The results are presented in Figure 1C. These data fit well to a model with a monomer-dimer equilibrium using three fitted parameters, the hydrodynamic radius $23.4 \pm 1 \text{ \AA}$ for the monomer, and $34.4 \pm 0.5 \text{ \AA}$ for the dimer, and a dissociation constant $K_d = 93 \pm 25 \mu\text{M}$ (Table 1).

The hydrodynamic radius obtained for the monomer of Sml1 is significantly smaller than the $R_H \approx 29.4 \text{ \AA}$ expected for an unstructured protein with the size of Sml1 (27). A folded monomer with mass 11.8 kDa is expected to have $R_H \approx 18.8 \text{ \AA}$. This suggests that the monomer of Sml1 exhibit some globular structure, but with few contributions from well defined secondary structure. This globularity is presumably due to intermittent tertiary interactions in the monomeric state. The expected hydrodynamic radius of a totally unfolded dimer with mass $2 \times 11834 \text{ Da}$ is 41 \AA and for a compactly folded dimer we expect $R_H \approx 23.2 \text{ \AA}$. The obtained value for the Sml1 dimer falls in between these calculated values. Assuming that the dimer is formed by two relatively unstructured monomers the expected increase in hydrodynamic radius is approximately $2^{1/2}$. The experimentally obtained increase is 1.47, and is in good agreement with the expected increase factor (27).

Size exclusion chromatography was used to also estimate the hydrodynamic dimensions of Sml1 (Figure 2S). Loading the column with high concentration leading to dilution on the column into both monomer and dimer, WT-Sml1 eluted as two peaks, corresponding to 33 \AA

and 23 Å, respectively, which is in good agreement with the results from the diffusion experiments.

Chemical shift analysis

Chemical shifts are very sensitive probes of secondary structure (29-32). One strategy in the chemical shift analysis is to compare the obtained chemical shifts with a reference value for a random coil. The chemical shift assignments were re-performed at high protein concentration (above 0.6 mM) with a dimer fraction of approximately 80 %.

The secondary chemical shifts analysis, Figure 2, suggests the presence of two helical regions in Sml1. One is located in the central part of the protein, and involves residues 60-86. A second region is located in the N-terminal part and includes residues 4-20 in agreement with previous observations (12). The maximum ^{15}N -secondary chemical shift in each helical region show a systematic four residues shift towards the C-terminus compared to the carbon shifts. This may indeed reflect hydrogen bonding between $\text{CO}_i - \text{H}^{\text{N}}_{i+4}$ as present in an α -helix. This has also been observed in the unfolded state of the all-helical protein ACBP (33). The effect is most prominent in the helical region of residues 60-86 but it is observed also in the N-terminal helix, and may reflect transient hydrogen bond formation. A third region of Sml1 involving residues 30-45 shows by both scales chemical shifts distinctly deviating from random coil shifts. This region exhibits a different behavior than the other two transient helical regions and it is not straightforward to conclude the precise nature of the transiently formed structure in this region.

In order to quantify the secondary structure propensity a secondary structure propensity (SSP) analysis were performed, following the procedure described by Marsh et al (34). The SSP analysis was performed using both the carbon shifts alone and using all available secondary chemical shifts and the results are shown in Figure 2, bottom panel. The SSP-analysis shows that the helix propensity in the region 60-80 is very high, and almost corresponds to a fully formed helix. Interestingly, the region 33-45 has SSP-values corresponding to β -sheet propensity. From the SSP-analysis the helix- and β -population may be estimated, and we found that Sml1 is 14% helical and has 2% β strand.

The chemical shift analysis of Sml1 does however not suggest a well defined structure, but rather shows localized populations of residual secondary structures in distinct parts of Sml1 in solution.

NMR relaxation

Regions with experimental evidence of populations adopting secondary structure are expected to exhibit slower dynamics than truly unfolded regions. The NMR relaxation phenomenon is directly linked to both the local and global dynamics of the protein (35-36). R_1 , R_2 ^{15}N NMR relaxation measurements combined with steady state heteronuclear ^{15}N NOEs were used to obtain information on the dynamical properties of Sml1. The relaxation rates and NOEs were determined at three different magnetic fields, 11.74, 14.09 and 18.79 T. The results from 14.09 T are shown in Figure 3. The average relaxation rates at the different fields are shown in Table 2.

The R_2 values reveal three regions with higher R_2 relaxation rates, and two of these regions are evident also in the R_1 data. The region involving residues 60-86 has the highest R_2 -values, as high as 13 s^{-1} at 14.09 T, but also the two N-terminal regions 4-20 and 25-45 exhibit relaxation faster than average with rates up to 11 s^{-1} . The NOE values are all above 0 and the pattern is similar as for the relaxation rates with higher NOE values for these three regions. Heteronuclear NOEs are very sensitive to local mobility, and reduced NOEs, i.e. larger values, typically indicate restricted motion. Taken together, these data indicate that the three regions

involving residues 4-20, 25-45 and 60-86 have less disorder and that they are separated by regions with higher mobility. The C-terminal end of the protein has a higher mobility than the N-terminus.

The dimerization interface

We studied the dimerization interface further using dilution series and induced spectral changes. Lowering the protein concentration drives the monomer-dimer equilibrium towards a higher monomer fraction. The induced chemical shift changes presumably reflect the regions of the protein that are involved in the dimerization. Figure 4 shows the induced chemical shift changes of the $^1\text{H}^{\text{N}}$ and ^{15}N resonances induced upon dilution of the sample from 480 μM to 30 μM , corresponding to a decrease of the dimer fraction from close to 0.7 to 0.2. Here one region shows significant changes, involving residues around residue 60 to residue 80, corresponding to the region with the highest helix propensity. There are also some general changes mainly involving the two regions centered on residues 10 and 35, also identified as regions with populations of transient structure. The sign of the chemical shift change suggest an increase in secondary structure propensity suggesting that dimer formation stabilizes the transient secondary structure.

The signal intensity change upon diluting Sml1 was also studied and the relative changes in signal intensity after dilution of Sml1 from 480 to 30 μM are shown in Figure 4B. The signal intensity is generally increased for the diluted sample suggesting a lower molecular weight and a faster overall tumbling rate. The region 45-60 however shows significant higher increase in intensity, suggesting that these regions exhibit a higher gain in mobility upon dissociation of the dimer. This region corresponds to the highly mobile region in between the more structured parts of Sml1.

Long range interactions in Sml1

Long range interactions in Sml1 were examined by the application of spin labeled Sml1 studied by paramagnetic relaxation enhancement (PRE) measurements. C14 was used to label the protein with MTSL, according to standard methods (26). ^1H , ^{15}N -HSQC spectra were recorded with the spin label in a paramagnetic and in a diamagnetic state, respectively. The cross-peak intensity changes are related to the relaxation enhancement which depends on the inverse sixth power of the distance between the amide nitrogen-proton vector and the spin label. Figure 5 shows the PREs calculated from the paramagnetic/diamagnetic ratios of the cross peak intensity per residue. As expected residues sequentially closest to the spin label are broadened beyond detection, but there are (at least) two additional regions that are affected, residues 60-70 and 85-95. For Sml1 the general broadening effect is closely correlated to the amide proton exchange rate and hence the peak intensity in the ^1H , ^{15}N -HSQC spectra. The two regions described above, however, fall outside this correlation and seem to originate from long range interactions within the protein (Supplementary Figure 1S).

To distinguish if the PREs observed are either intra- or intermolecular, spin labeled ^{14}N -Sml1 was mixed with ^{15}N -Sml1 without spin label. No significant line broadening was observed in the ^{15}N -Sml1 HSQC spectrum suggesting strongly that the observed spin label induced PREs are intramolecular. Interesting, changes in chemical shifts on ^{15}N -Sml1 as a result of reduction of the MTSL label on ^{14}N -Sml1 were however observed for residues around 70. This suggests that this region may be involved both in intra and inter-molecular interactions within Sml1 (data not shown).

A rigorous treatment of the PRE data should include several spin-label positions as well as an ensemble simulation (37). The present data suffers from the fact that the spin-label has only been introduced at one site of the protein, i.e. at the single native cysteine, C14. However, the

PRE data are in good agreement with our results obtained from other methods. As seen directly from the PRE data the N-terminus is close to two regions in the C-domain. This indicates that Sml1 has a transient overall folded structure where the N-terminal domain folds onto and caps the C-domain. This is in agreement with the relatively small hydrodynamic radius of Sml1 (23.4 Å) measured by diffusion, as described above.

NMR studies of a truncated variant of Sml1

The N-terminal domain may be defined to consist of residues 1-49 and the C-terminal domain to consist of residues 50-104. The C-terminal fragment Sml1(50-104) was obtained and studied by NMR, both in order to determine the oligomeric state and to measure the transient secondary structure population of this inhibitory effective fragment.

The nitrogen secondary chemical shifts of Sml1(50-104) showed a similar pattern as the C-terminal domain of the full length WT Sml1. The C-terminal fragment has a high population of transient helical structure in a region spanning residues 53-70, suggesting that Sml1(50-104) has similar helical properties as in the wild type protein. The transient helical region has similar length in wild type and Sml1(50-104), while the region is shifted towards the N-terminus in Sml1(50-104) (data not shown).

To define the oligomeric state of Sml1 (50-104) the concentration dependence of the translational diffusion coefficient was studied. The dimerization of WT Sml1 was shown above to involve residues in both the N-terminal and C-terminal part of Sml1, and thus the fragment (50-104) was not expected to form dimers with the same specificity as the wild type. Figure 1B also shows that the diffusion coefficient of Sml1(50-104) displays only weak concentration dependence. The diffusion coefficient of Sml1(50-104) corresponds to a hydrodynamic radius $R_H = 19.9 \text{ \AA}$, and suggests that Sml1(50-104) has a more extended, random structure with some transient secondary structure regions, as shown with chemical shift analysis.

The central helical region involving residues 60-86 is crucial for Sml1 inhibition of RNR R1 (12) and this give rise to the question of the role of the N-terminal domain, if not important for function. The N-terminal domain has two regions with significant populations of secondary structure which suggest that also this domain has a role in Sml1 overall function.

Protease resistance of Sml1 and Sml1(50-104)

In order to study the importance of the N-terminal domain of wild type Sml1 we performed protease degradation studies of both the wild type Sml1 and the N-terminally truncated variant, both at monomeric and dimeric concentrations. In separate studies protease K or trypsin were added to stock solutions of Sml1 or of Sml1(50-104) at low protein concentration. The degradation of the proteins were followed over time and analyzed by SDS-PAGE and MALDI-TOF mass-spectrometry (MS), Figure 6. The degradation produces several distinct fragments, manifested as clear-cut bands in the gel, Figure 6A. It is clear that the degradation resistance of the wild type Sml1 is significantly stronger than for the shorter variant and we qualitatively estimate the degradation time to be at least four times the degradation time of the truncated variant Sml1(50-104), Figure 6A. From the limited trypsin digestion of wild type Sml1, we observe fragments resulting only from the N-terminal domain, whereas fragment resulting from cleavage in the C-terminal domain were not seen. For the Sml1(50-104) we distinctly observe degradation fragments resulting from cleavage in the C-domain, which were not observed for wild type Sml1 at the same time point, Figure 6C. Independently, the protease K and the trypsin digestion data suggest that the N-terminal domain protects the C-domain of Sml1 from degradation and may provide an explanation as to why the N-terminal region has been conserved in evolution.

We also performed degradation studies of the full length protein at two different concentrations to determine the effect of dimerization on the degradation rate. Figure 6B shows the degradation of wild type Sml1 at 20 and 200 μ M corresponding to approximately 20 and 60 % of Sml1 dimers, respectively. The degradation of the sample with high dimer concentration is significantly slower as seen when comparing qualitatively the intensities of the degradation fragment bands to the non-degraded band intensity. The low concentration sample Sml1 (mainly monomeric) degrades approximately four times faster than the high concentration sample Sml1 (mainly dimers), suggesting that the formation of dimers significantly protects the protein from degradation. Apart from delayed degradation, the only difference in the cleavage patterns in relation to dimerisation as analyzed by limited trypsin digestion and MALDI-TOF MS was seen at residue 13, which was only observable as cleavage point at low protein concentration.

DISCUSSION

We present here a structural characterization of the intrinsically unfolded protein Sml1 and show that even in the absence of well defined secondary structures, Sml1 adopts a tertiary and globular fold where the N-terminal domain folds onto and caps the C-terminal domain in a protease protective way. A structural sketch is shown in Figure 7. For the sake of clearness we represent the transient structural regions as pronounced lines and we refer to these regions as helical or structured, although these structural elements are highly transient.

The hydrodynamic radius of Sml1 as determined by PFG-NMR and size exclusion chromatography suggests that Sml1 does not behave as a random coil or as an extended unfolded protein. The small hydrodynamic radius suggests that Sml1 adopts a loosely folded structure. This is in agreement with earlier suggestions that Sml1 adopts a loose overall tertiary structure (12,20). This is also supported by the PRE data which indicate long range contacts between the N-terminal domain and the regions 60-80 and 85-95, and is also suggested from the chemical shift analysis of the 50-104 fragment. There is no evidence of a well defined overall structure and we suggest transient but specific capping of the C-domain by the N-domain. The PRE data of disordered proteins shall be interpreted with caution. The distances in a highly mobile system should be considered as distributions of distances rather than fixed distances. Also, the amide proton relaxation rates and the amide proton exchange rates are expected to vary significantly along the polypeptide chain in a highly dynamical protein. The amide proton exchange rate is reflected by the signal intensity in the HSQC spectrum, and we used this effect to be able to separate the significant PREs from those mainly affected by amide proton exchange effects. Despite all these interpretation problems arising from the dynamic features of a disordered protein, the PRE data is in good agreement with the relaxation and diffusion data, and thus the two long range contact regions found here are considered significant.

The induced changes in chemical shifts upon dimerization as shown in Figure 4 suggest that the dimerization does not induce any significant change in the monomeric structure of Sml1. Our findings that the most affected residues 60-80 is involved in specific dimerization is in apparent disagreement with earlier findings that the dimerization site is located in the 1-20 region (13). However, as the N-terminal domain, and especially the helical region 4-20, is important for the overall fold of Sml1, as described above, deletion of this region can be expected to affect dimerization indirectly. This suggests that the N-terminal region of Sml1 is important for dimerization. However, the largest impact on chemical shifts is seen in the region 60-80, and we therefore proposes the following model; for specific dimerization-interactions to occur Sml1 has to fold, i.e. the N-terminal has to cap the C-terminal. The dimerization leads to stabilization of the transient secondary structures of Sml1. The dimerization together with

the induced stabilization then restricts the mobility of the flexible region 45-60, leading to a reduction in NMR signal intensity from these residues.

We were able to show that both the dimerization and the N-domain capping of the C-domain protect Sml1 from degradation. The N-terminal domain capping decreases the degradation rate by a factor of four and protects specific cleavage sites in the C-domain as seen by MALDI-TOF MS. This leads to a model where the C-domain is the inhibition domain and the N-domain is a shield, a molecular aegis, for the functional sites, protecting these from degradation. Dimerization serves an additional and significant protection from protease degradation. This is interesting and to our knowledge a novel finding, since functional dimerization giving rise to protection from degradation has hitherto not been frequently observed in IDPs, although non-functional dimerization has been observed (38), as well as disordered proteins that fold upon dimerization (39). In a recent paper Simon et al. show that the IDP UmuD2 forms stable homo-dimers, however with significant gain of structure (40). This is in contrast to what we observe here. We propose that the molecular shielding and protection of vital functional structures from degradation by functionally unimportant sites may be a general attribute of others IDPs.

The protective role of the N-terminal may be used in the regulation of Sml1 function by the yeast cell. When RNR activity is needed, e.g. as a response to DNA damage, phosphorylation of serines 56, 58 and/or 60 is induced. This may perturb long range interactions within Sml1 and increase degradation which results in an increased amount of free, active RNR. This strategy to use phosphorylation as a regulation has been shown also in other unfolded proteins (10 and references therein).

Our data leads to a model of Sml1 function and provides an explanation for the observation that Sml1 forms dimers. The dissociation constant for Sml1 dimerization is relatively high suggesting that the biological relevance may be questioned. However, at translation the local concentration of Sml1 may be high enough to promote dimerization and this may then be an effective protection against degradation directly after translation. After translation Sml1 can be assumed to be more diluted and this may shift the equilibrium towards a higher population of monomers. In order to protect against degradation the N-terminal domain is folded onto the C-terminal domain. However, the C-domain may have to be uncapped in order to be able to bind specifically to the subunit R1 of RNR. This may provide an explanation to why the protein does not form a tight and well-defined structure. In order to enable interaction between the helical region (60-86) and the binding site on R1, the N-domain may need to rearrange and expose the helical region.

Supplementary Material

Refer to Web version on PubMed Central for supplementary material.

ACKNOWLEDGMENTS

We wish to thank Lars Thelander and Vladimir Domkin for fruitful discussions and Signe Agernæs Sjørup for skilled technical assistance. We acknowledge the points raised by the reviewers concerning the dimerisation process.

FUNDING: This work was supported in part by the Carlsberg Foundation (FMP) and the Danish Natural Research Councils (#21040604; BBK).

ABBREVIATIONS

Sml1, suppressor of Mec1 lethality
RNR, ribonucleotide reductase

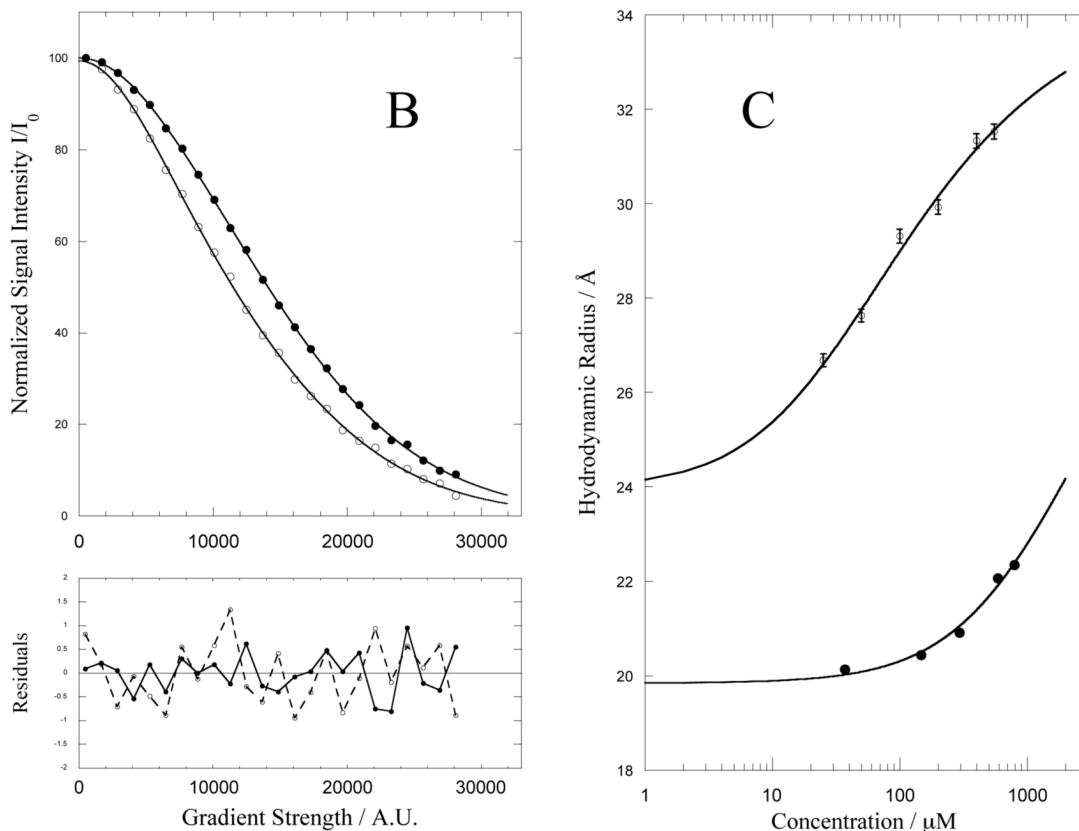
IDP, intrinsically disordered protein
 NMR, nuclear magnetic resonance
 HSQC, heteronuclear single quantum correlation
 PFG, pulsed field gradient
 NOE, nuclear Overhauser effect
 SSP, secondary structure propensity
 PRE, paramagnetic relaxation enhancement
 MTSL, (1-oxy-2,2,5,5-tetramethyl-3-pyrroline-3-methyl)-methanethiosulfonate
 MS, mass-spectrometry

REFERENCES

1. Chabes A, Domkin V, Larsson G, Liu A, Gräslund A, Wijmenga S, Thelander L. Yeast ribonucleotide reductase has a heterodimeric iron-radical-containing subunit. *Proc. Natl. Acad. Sci. U. S. A* 2000;97:2474–2479. [PubMed: 10716984]
2. Gräslund A, Sahlin M. Electron paramagnetic resonance and nuclear magnetic resonance studies of class I ribonucleotide reductase. *Annu. Rev. Biophys. Biomol. Struct* 1996;25:259–286. [PubMed: 8800471]
3. Chabes A, Domkin V, Thelander L. Yeast Sml1, a protein inhibitor of ribonucleotide reductase. *J. Biol. Chem* 1999;274:36679–36683. [PubMed: 10593972]
4. Zhao X, Muller EGD, Rothstein R. A suppressor of two essential checkpoint genes identifies a novel protein that negatively affects dNTP pools. *Mol. Cell* 1998;2:329–340. [PubMed: 9774971]
5. Zhao X, Chabes A, Domkin V, Thelander L, Rothstein R. The ribonucleotide reductase inhibitor Sml1 is a new target of the Mec1/Rad53 kinase cascade during growth and in response to DNA damage. *EMBO J* 2001;20:3544–3553. [PubMed: 11432841]
6. Zhao X, Rothstein R. The Dun1 checkpoint kinase phosphorylates and regulates the ribonucleotide reductase inhibitor Sml1. *Proc. Natl. Acad. Sci. U. S. A* 2002;99:3746–3751. [PubMed: 11904430]
7. Uchiki T, Dice LT, Hettich RL, Dealwis C. Identification of phosphorylation sites on the yeast Ribonucleotide Reductase inhibitor Sml1. *J. Biol. Chem* 2004;279:11293–11303. [PubMed: 14684746]
8. Elledge SJ. Cell cycle checkpoints: preventing an identity crisis. *Science* 1996;274:1664–1671. [PubMed: 8939848]
9. Taylor SD, Zhang H, Eaton JS, Rodeheffer MS, Lebedeva MA, O'Rourke TW, Siede W, Shadel GS. The conserved Mec1/Rad53 nuclear checkpoint pathway regulates mitochondrial DNA copy number in *Saccharomyces cerevisiae*. *Mol. Biol. Cell* 2005;16:3010–3018. [PubMed: 15829566]
10. Dyson HJ, Wright PE. Intrinsically unstructured proteins and their functions. *Nat. Rev. Mol. Cell. Biol* 2005;6:197–208. [PubMed: 15738986]
11. Wright PE, Dyson HJ. Intrinsically unstructured proteins: re-assessing the protein structure-function paradigm. *J. Mol. Biol* 1999;293:321–331. [PubMed: 10550212]
12. Zhao X, Georgieva B, Chabes A, Domkin V, Ippel JH, Schleucher J, Wijmenga S, Thelander L, Rothstein R. Mutational and structural analyses of the ribonucleotide reductase inhibitor Sml1 define its Rnr1 interaction domain whose inactivation allows suppression of mec1 and rad53 lethality. *Mol. Cell. Biol* 2000;20:9076–9083. [PubMed: 11074005]
13. Gupta V, Peterson CB, Dice LT, Uchiki T, Racca J, Guo J-T, Ying X, Hettich R, Zhao X, Rothstein R, Dealwis CG. Sml1p is a dimer in solution: characterization of denaturation and renaturation of recombinant Sml1p. *Biochemistry* 2004;43:8568–8578. [PubMed: 15222768]
14. Dyson HJ, Wright PE. Insights into the structure and dynamics of unfolded proteins from nuclear magnetic resonance. *Adv. Protein Chem* 2002;62:311–340. [PubMed: 12418108]
15. Dyson HJ, Wright PE. Unfolded proteins and protein folding studied by NMR. *Chem. Rev* 2004;104:3607–3622. [PubMed: 15303830]
16. Uversky VN. What does it mean to be natively unfolded? *Eur. J. Biochem* 2002;269:2–12. [PubMed: 11784292]
17. Vendruscolo M, Dobson CM. A glimpse at the organization of the protein universe. *Proc. Natl. Acad. Sci. U. S. A* 2005;102:5641–5642. [PubMed: 15827120]

18. Frieden C, Chattopadhyay K, Elson EL. What fluorescence correlation spectroscopy can tell us about unfolded proteins. *Adv. Protein Chem* 2002;62:91–109. [PubMed: 12418102]
19. Keiderling TA, Xu Q. Unfolded peptides and proteins studied with infrared absorption and vibrational circular dichroism spectra. *Adv. Protein Chem* 2002;62:111–161. [PubMed: 12418103]
20. Sharp JS, Guo J-T, Uchiki T, Xu Y, Dealwis C, Hettich R. Application of photochemical surface mapping of C16S Sml1p to constrained computational modeling. *Anal. Biochem* 2005;340:201–212. [PubMed: 15840492]
21. Kjær M, Andersen KV, Poulsen FM. Automated and semiautomated analysis of homo- and heteronuclear multidimensional nuclear magnetic resonance spectra of proteins: the program Pronto. *Meth. Enzymol* 1994;239:288–307. [PubMed: 7830586]
22. Gibbs SJ, Johnson CS. A PFG NMR experiment for accurate diffusion and flow studies in the presence of eddy currents. *J. Magn. Reson* 1991;93:395–402.
23. Yao S, Howlett GJ, Norton RS. Peptide self-association in aqueous trifluoroethanol monitored by pulsed field gradient NMR diffusion measurements. *J. Biomol. NMR* 2000;16:109–119. [PubMed: 10723990]
24. Stejskal EO, Tanner JE. Spin diffusion measurements: spin echoes in the presence of a time dependent field gradient. *J. Chem. Phys* 1965;42:288–292.
25. Damberg P, Jarvet J, Gräslund A. Accurate measurement of translational diffusion coefficients: a practical method to account for nonlinear gradients. *J. Magn. Reson* 2001;148:343–348. [PubMed: 11237640]
26. Teilum K, Kragelund BB, Poulsen FM. Transient structure formation in unfolded acyl-coenzyme A-binding protein observed by site-directed spin labelling. *J. Mol. Biol* 2002;324:349–357. [PubMed: 12441112]
27. Danielsson J, Jarvet J, Damberg P, Gräslund A. Translational diffusion measured by PFG-NMR on full length and fragments of the Alzheimer A β (1-40) peptide. Determination of hydrodynamic radii of random coil peptides of varying length. *Magnet. Reson. Chem* 2002;40:S89–S97.
28. Wilkins DK, Grimshaw SB, Receveur V, Dobson CM, Jones JA, Smith LJ. Hydrodynamic radii of native and denatured proteins measured by pulse field gradient NMR techniques. *Biochemistry* 1999;38:16424–16431. [PubMed: 10600103]
29. Berjanskii MV, Wishart DS. The RCI server: rapid and accurate calculation of protein flexibility using chemical shifts. *Nucleic Acids Res* 2007;35:W531–W537. [PubMed: 17485469]
30. Berjanskii MV, Wishart DS. Application of the random coil index to studying protein flexibility. *J. Biomol. NMR* 2008;40:31–48. [PubMed: 17985196]
31. Schwarzinger S, Kroon GJA, Foss TR, Chung J, Wright PE, Dyson HJ. Sequence-dependent correction of random coil NMR chemical shifts. *J. Am. Chem. Soc* 2001;123:2970–2978. [PubMed: 11457007]
32. Wishart DS, Sykes BD. Chemical shifts as a tool for structure determination. *Meth. Enzymol* 1994;239:363–392. [PubMed: 7830591]
33. Modig K, Juergensen VW, Lindorff-Larsen K, Fieber W, Bohr HG, Poulsen FM. Detection of initiation sites in protein folding of the four helix bundle ACBP by chemical shift analysis. *FEBS Lett* 2007;581:4965–4971. [PubMed: 17910956]
34. Marsh JA, Singh VK, Jia Z, Forman-Kay JD. Sensitivity of secondary structure propensities to sequence differences between {alpha}- and {gamma}-synuclein: Implications for fibrillation. *Protein Sci* 2006;2795–2804. [PubMed: 17088319]
35. Lipari G, Szabo A. Model-free approach to the interpretation of nuclear magnetic resonance relaxation in macromolecules. 1. Theory and range of validity. *J. Am. Chem. Soc* 1982;104:4546–4559.
36. Lipari G, Szabo A. Model-free approach to the interpretation of nuclear magnetic resonance relaxation in macromolecules. 2. Analysis of experimental results. *J. Am. Chem. Soc* 1982;104:4559–4570.
37. Lindorff-Larsen K, Kristjansdottir S, Teilum K, Fieber W, Dobson CM, Poulsen FM, Vendruscolo M. Determination of an ensemble of structures representing the denatured state of the bovine acyl-coenzyme A binding protein. *J. Am. Chem. Soc* 2004;126:3291–3299. [PubMed: 15012160]
38. Fieber W, Kragelund BB, Meldal M, Poulsen FM. Reversible dimerization of acid-denatured ACBP controlled by helix A4. *Biochemistry* 2005;44:1375–1384. [PubMed: 15683223]

39. Song J, Guo L-W, Muradov H, Artemyev NO, Ruoho AE, Markley JL. Intrinsically disordered γ - subunit of cGMP phosphodiesterase encodes functionally relevant transient secondary and tertiary structure. *Proc. Natl. Acad. Sci. U. S. A* 2008;105:1505–1510. [PubMed: 18230733]
40. Simon SM, Sousa FJR, Mohana-Borges R, Walker GC. Regulation of *Escherichia coli* SOS mutagenesis by dimeric intrinsically disordered *umuD* gene products. *Proc. Natl. Acad. Sci. U. S. A* 2008;105:1152–1157. [PubMed: 18216271]
41. Zhang H, Neal S, Wishart DS. RefDB: A database of uniformly referenced protein chemical shifts. *J Biomol NMR* 2003;25:173–195. [PubMed: 12652131]



A

MQNSQDYFYA₁₀ QNRCQQQQAP₂₀ STLRTVTMAE₃₀ FRRVPLPPMA₄₀
 EVPMLSTQNS₅₀ MGSSASASAS₆₀ SLEMWEKDLE₇₀ ERLNSIDHDM₈₀
 NNNKFGSGEL₉₀ KSMFNQ GKVE₁₀₀ EMDF

Figure 1. Hydrodynamic radii of Sml1

(A). Amino acid sequence of Sml1. (B) Signal attenuation curves from ^1H -PFG-NMR translational diffusion measurements of Sml1 at two different concentrations, filled circles; 550 μM , open circles; 25 μM , at 278 K. The lower panel shows the residuals after fitting attenuation data to the modified Stejskal-Tanner equation described in the method section. (C) The concentration dependence of the hydrodynamic radius, calculated from the diffusion coefficients, of the full length wild type Sml1 (open circles) and the truncated Sml1(50-104) (closed circles). The curves are generated from a simple two-state model where three parameters are fitted, $R_{\text{H}}(\text{monomer})$, $R_{\text{H}}(\text{dimer})$ and K_{D} .

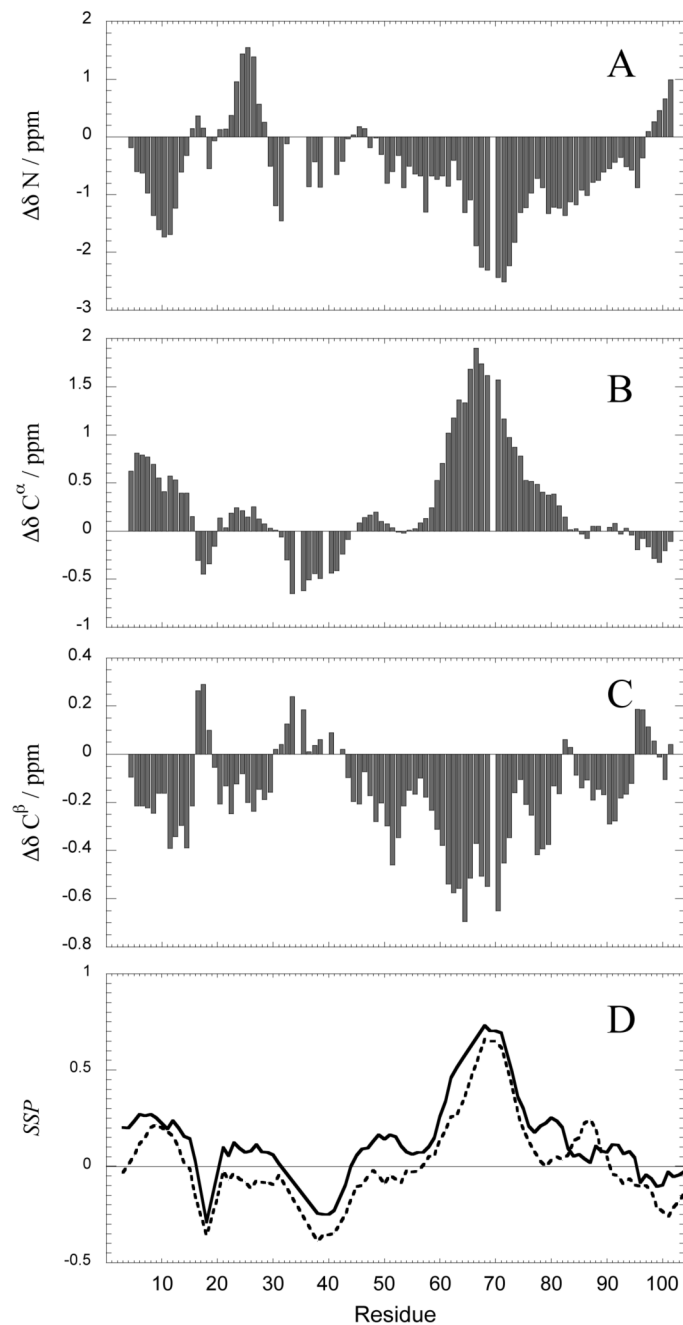


Figure 2. Secondary chemical shifts

(A-C) Secondary chemical shift of Sml1 relative to random coil values (41). (D) SSP-analysis performed as described by Marsh et al. (34). Values close to 1 corresponds to fully formed α -helix and values close to -1 correspond to fully formed α -sheet.

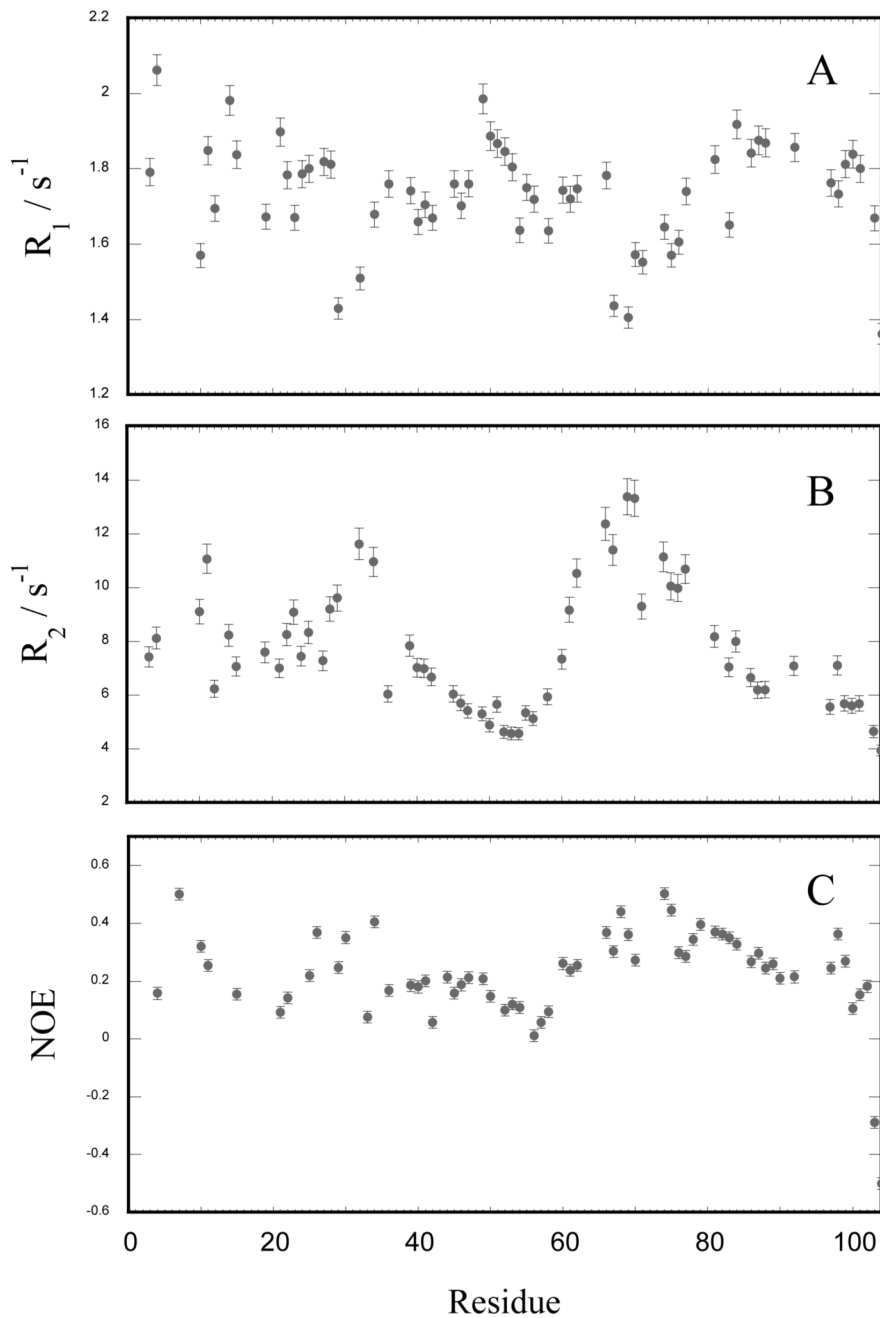


Figure 3. Relaxation properties of Sml1

^{15}N -relaxation data of 0.7 mM Sml1, pH 7.2 in 10 mM phosphate buffer, 278 K. The data shown are R_1 , R_2 and NOE at 600 MHz proton frequency. Missing data points are due to poor resolution and/or unstable data fit.

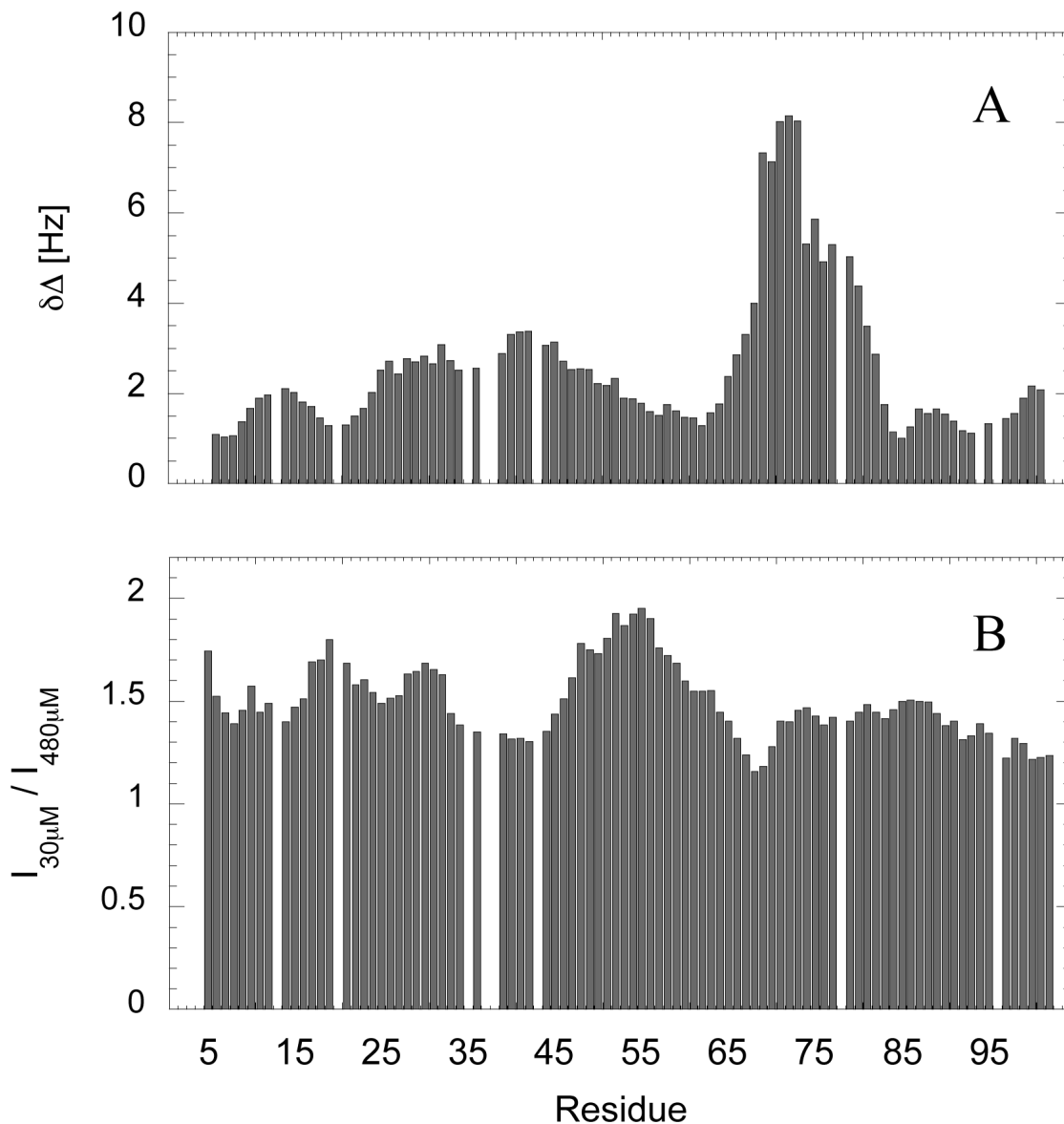


Figure 4. Dimerization interface of Sm11

(A). Induced chemical shift changes of $^1\text{H}^{\text{N}}$ and ^{15}N upon dilution of Sm11 from 0.48 mM to 30 μM in 10 mM phosphate buffer, pH 7.2, 278 K. The values are averaged over 5 residues. The most prominent changes are seen in the region involving residues 60-80, suggesting involvement in the dimerization, but also residues in the region of the N-terminal helix are affected. (B) The relative change in signal intensity upon dilution of the sample from 0.48 mM to 30 μM . The values are averaged over 5 residues. Here the highly mobile region 45-60 is most affected suggesting that this region increases its mobility upon dissociation from dimeric to monomeric state.

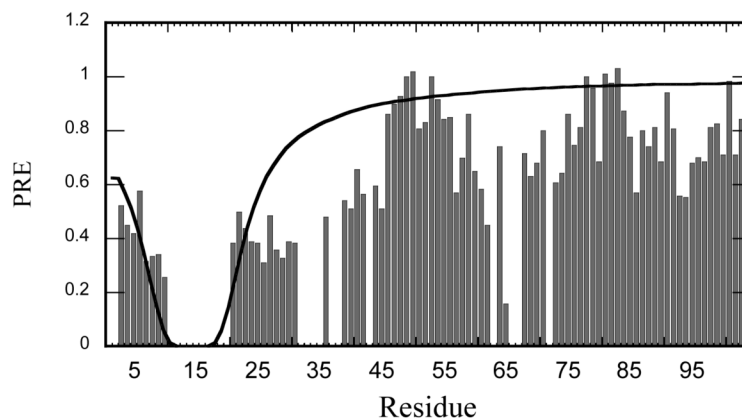


Figure 5. Long-range interactions in Sml1

Paramagnetic relaxation enhancement of Sml1 after selective spin labeling of C14 with MTSL. Two regions show long range interactions with the N-terminal, the regions 60-75 and 85-95. The solid line represents the expected value of the PREs for a Gaussian random coil. This was calculated by creating 10000 gaussian excluded volume bead-on-a-string chains, with an excluded volume diameter $D_V=5 \text{ \AA}$, parameterised to yield hydrodynamic radius corresponding to a classic random coil.

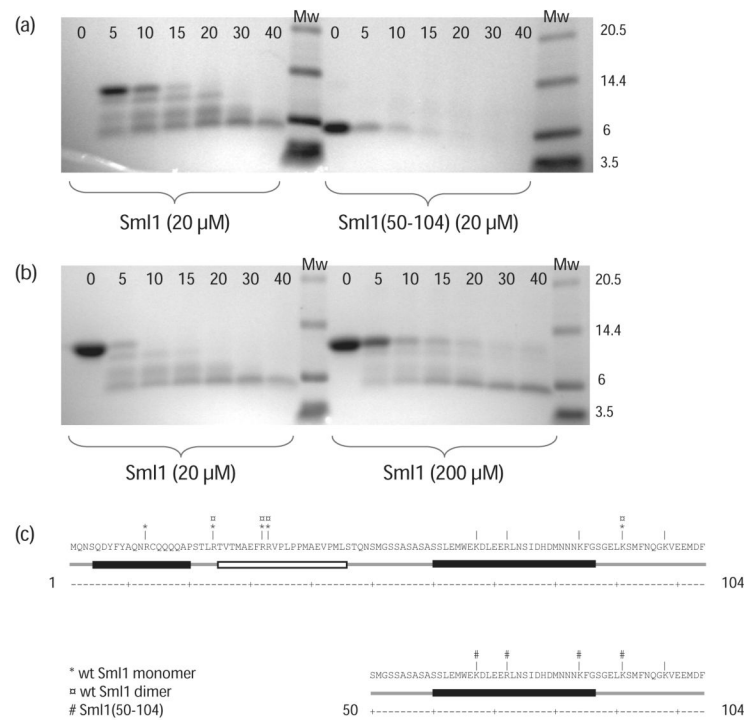


Figure 6. Protection of Sml1 from protease degradation

SDS-PAGE following the Protease K degradation of (A) wild type Sml1 and Sml1(50-104) at 20 μM as a function of time (minutes), showing slower degradation rate for the full length protein when compared to the N-terminally truncated Sml1(50-104). Note that the first time point for the wt Sml1 is missing due to precipitation (B) Sml1 at two different concentrations corresponding to a high (200 μM, 69% dimer) and a low (20 μM, 31 % dimer) population of dimers. The degradation experiment shows that the dimer is significantly slower degraded suggesting that dimerization also protects the protein from degradation. (C) Tryptic cleavage sites in Sml1(monomer), Sml1(50-104) and Sml1(dimer) as observed by MALDI-TOF MS from limited trypsin digestion at 40 min of reaction. Possible trypsin cleavage sites in the sequences are indicated with vertical lines above the residues. *sites observed in monomeric Sml1 at 20 μM, □ sites observed in dimeric Sml1 (200 μM) and # sites observed in Sml1 (50-104) at 20 μM. The lines below the sequences show partial structured region with helix populations marked in black and mixed structure in white.

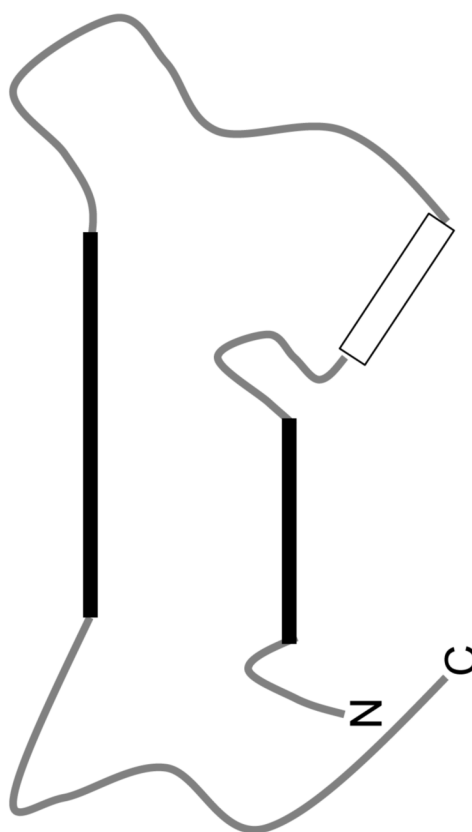


Figure 7. A naïve structural model of Sml1

A simple structural sketch of the backbone of Sml1 providing a naïve model which is in agreement with present data. The lines show partial structured region with helix populations marked in black and mixed structure in white. The structural propensities are not absolute, and thus, we choose to represent the structure using this naïve model.

TABLE 1

Measured and theoretically estimated (21) hydrodynamic radii of monomeric and dimeric Sml1.

	Monomer [Å]	Dimer [Å]
Experimental	23.4	34.4
Theoretical unfolded	29.4	41
Theoretical folded	18.8	23.2

TABLE 2

Relaxation data. Averaged relaxation data for R1 and R2 at the three magnetic fields.

Magnetic field (T)	R ₁ (s ⁻¹)	R ₂ (s ⁻¹)
11.74	1.8 ± 0.1	7.4 ± 2.7
14.09	1.8 ± 0.2	8.4 ± 2.9
18.79	1.7 ± 0.2	9.4 ± 3.4